

See discussions, stats, and author profiles for this publication at: <https://www.researchgate.net/publication/11164597>

# Substituted Polypyridine Complexes of Cobalt(II/III) as Efficient Electron-Transfer Mediators in Dye-Sensitized Solar Cells

ARTICLE in JOURNAL OF THE AMERICAN CHEMICAL SOCIETY · OCTOBER 2002

Impact Factor: 12.11 · DOI: 10.1021/ja027355y · Source: PubMed

---

CITATIONS

334

---

READS

132

5 AUTHORS, INCLUDING:



Stefano Caramori

University of Ferrara

49 PUBLICATIONS 1,524 CITATIONS

SEE PROFILE



Carlo Alberto Bignozzi

University of Ferrara

203 PUBLICATIONS 8,672 CITATIONS

SEE PROFILE

## Substituted Polypyridine Complexes of Cobalt(II/III) as Efficient Electron-Transfer Mediators in Dye-Sensitized Solar Cells

Shawn A. Sapp,<sup>†</sup> C. Michael Elliott,<sup>\*,†</sup> Cristiano Contado,<sup>‡</sup> Stefano Caramori,<sup>‡</sup> and Carlo A. Bignozzi<sup>\*,‡</sup>

*Contribution from the Department of Chemistry, Colorado State University, Fort Collins, Colorado 80523-1872*

Received June 18, 2002

**Abstract:** A number of cobalt complexes of substituted polypyridine ligands were synthesized and investigated as possible alternatives to the volatile and corrosive iodide/triiodide redox couple commonly used as an electron-transfer mediator in dye-sensitized solar cells (DSSCs). The extinction coefficients in the visible spectrum are on the order of  $10^2 \text{ M}^{-1} \text{ cm}^{-1}$  for the majority of these complexes, diminishing competition with the light-harvesting dye. Cyclic voltammetric studies revealed a dramatic surface dependence of the heterogeneous electron-transfer rate, which is surprisingly different for gold, carbon, and platinum electrodes. DSSCs were assembled using a mediator that consisted of a mixture of Co(II) and Co(III) complexes in a 10:1 ratio. DSSCs containing these mediators were used to characterize incident photon-to-current conversion efficiency and photoelectrochemical responses. The best performing of these mediators were identified and subjected to further study. As suggested by electrochemical results, gold and carbon are superior cathode materials to platinum, and no evidence of corrosion on any cathode material was observed. Addition of lithium salts to the mediator solution resulted in a dramatic improvement in cell performance. The observed  $\text{Li}^+$  effect is explained in terms of the recombination of injected electrons in the photoanode with the oxidized mediator. The best mediator, based on tris(4,4'-di-*tert*-butyl-2,2'-dipyridyl)-cobalt(II/III) perchlorate, resulted in DSSCs exhibiting efficiencies within 80% of that of a comparable iodide/triiodide-mediated DSSC. Due to the commercial availability of the ligand and the simplicity with which the complex can be made, this new mediator represents a nonvolatile, noncorrosive, and practical alternative as an efficient electron-transfer mediator in DSSCs.

### Introduction

It is now well-documented that certain photoelectrochemical cells based on dye-sensitized nanocrystalline  $\text{TiO}_2$  photoanodes can have total energy conversion efficiency in excess of 10% when irradiated with sunlight.<sup>1</sup> Such efficiencies meet or exceed those of solid-state cells based on amorphous silicon but fall far short of the efficiency of single crystal and polycrystalline silicon cells.<sup>2–4</sup> That fact notwithstanding, the potential for fabricating large surface area cells out of relatively inexpensive materials—compared to single crystalline silicon cells, for example—is driving interest in dye-sensitized solar cells (DSSCs).

While the demonstrated energy conversion efficiencies of DSSCs have become competitive with some existing commercial technologies, there are a number of issues that remain

to be addressed before this type of cell can become truly commercially viable. The first issue is that the best “dyes” for sensitizing the  $\text{TiO}_2$  photoanode are ruthenium-based coordination complexes. With such dyes there are potential stability issues. Furthermore, ruthenium is relatively rare, and major known sources are geographically localized in politically unstable regions; thus, its use could pose serious practical problems. Second, only cells based on liquid-state electrolytes have produced the high efficiencies required for competitiveness with existing technologies.<sup>5–9</sup> Last, an extremely limited set of electron-transfer mediators work in these cells. The overall best system to date is the  $\text{I}^-/\text{I}_3^-$  couple, which regrettably has a list of undesirable chemical properties.<sup>10</sup>

Considerable effort has been focused on finding new dyes.<sup>11</sup> In contrast, efforts to find electron-transfer mediators other than

\* Authors for correspondence. E-mail: elliotl@lamar.colostate.edu and g4s@unife.it.

<sup>†</sup> Department of Chemistry, Colorado State University, Fort Collins, CO 80523.

<sup>‡</sup> Dipartimento di Chimica, Università di Ferrara, 44100 Ferrara, Italy.

(1) Nazeeruddin, M. K.; Pechy, P.; Renouard, T.; Zakeeruddin, S. M.; Humphry-Baker, R.; Comte, P.; Liska, P.; Cevey, L.; Costa, E.; Shklover, V.; Spiccia, L.; Deacon, G. B.; Bignozzi, C. A.; Gratzel, M. *J. Am. Chem. Soc.* **2001**, *123*, 1613.

(2) Green, M. A. *MRS Bull.* **1993**, *18*, 26.

(3) Watanabe, H. *MRS Bull.* **1993**, *18*, 29.

(4) Hamakawa, Y.; Ma, W.; Okamoto, H. *MRS Bull.* **1993**, *18*, 38.

(5) Cao, F.; Oskam, G.; Searson, P. C. *J. Phys. Chem.* **1995**, *99*, 17071.

(6) Papageorgiou, N.; Athanassov, Y.; Armand, M.; Bonhote, P.; Pettersson, H.; Azam, A.; Gratzel, M. *J. Electrochem. Soc.* **1996**, *143*, 3099.

(7) Murakoshi, K.; Kogure, R.; Wada, Y.; Yanagida, S. *Chem. Lett.* **1997**, 471.

(8) Murakoshi, K.; Kogure, R.; Wada, Y.; Yanagida, S. *Sol. Energy Mater. Sol. Cells* **1998**, *55*, 113.

(9) Savenije, T. J.; Warman, J. M.; Goossens, A. *Chem. Phys. Lett.* **1998**, *287*, 148.

(10) Gregg, B. A.; Pichot, F.; Ferrere, S.; Fields, C. L. *J. Phys. Chem. B* **2001**, *105*, 1422.

(11) Hagfeldt, A.; Gratzel, M. *Acc. Chem. Res.* **2000**, *33*, 269.

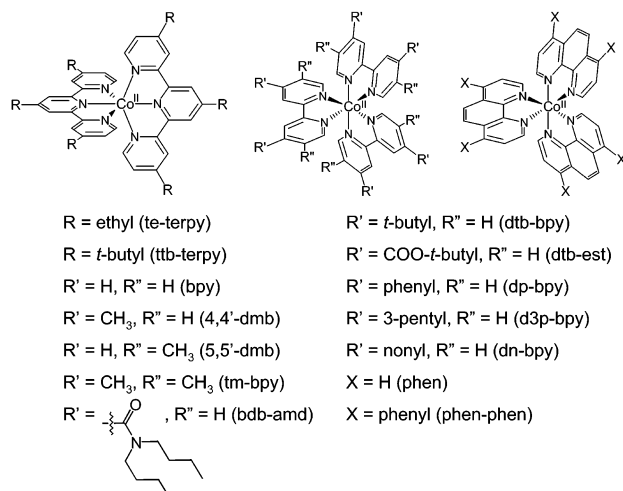


**Figure 1.** Series of terpyridine, bipyridine, and phenanthroline complexes of cobalt(II) synthesized and employed in this study. The abbreviated names, as used in the text, refer to the entire complex, not to the ligands.

$\text{I}^-/\text{I}_3^-$  have been relatively modest.<sup>10,12</sup> The  $\text{I}^-/\text{I}_3^-$  couple functions well in these cells because of a fortunate confluence of the right kinetics for at least four different heterogeneous electron-transfer reactions: (1) The photoexcited dye must inject an  $e^-$  faster than it reacts with the mediator. (2) The oxidized dye must be reduced by the mediator more rapidly than it recombines with the photoinjected electron. (3) The oxidized mediator must, itself, react slowly with electrons in both the  $\text{TiO}_2$  and the fluorine-doped tin oxide ( $\text{SnO}_2:\text{F}$ ) contact. (4) Finally, the reduction of the oxidized mediator at the cathode must be rapid. At present, there is no way to predict what other systems might possess similar electron-transfer kinetics—which is most likely why this problem has been less aggressively addressed.

Periodically, interest arises in cobalt complexes as mediators in DSSCs, but many previous efforts along these lines have been disappointing.<sup>13,14</sup> There has also been a report of a cobalt complex-based mediator that rivaled the  $\text{I}^-/\text{I}_3^-$  mediator in terms of the kinetics to regenerate the dye.<sup>15</sup> However, the ligands used to form this complex are not readily available, and we assume were obtained using a multistep synthetic procedure.<sup>15</sup>

We have recently discovered that particular cobalt polypyridine complexes—formed from structurally simple ligands—do function as efficient electron-transfer mediators in DSSCs. Figure 1 shows the structures of a series of cobalt–polypyridine complexes synthesized in our labs to identify what structural and thermodynamic motifs generate the best mediators. The focus of this investigation was not to generate the highest-efficiency cells possible but rather to generate cells with cobalt complex mediators that closely match the performance of comparable  $\text{I}^-/\text{I}_3^-$  mediated cells. In the best case thus far, the cobalt-based mediators reported here give efficiencies greater

than 80% of that given by the comparable cell mediated by the  $\text{I}^-/\text{I}_3^-$  couple.

## Experimental Section

**Materials.** Acetonitrile (Fisher Optima Grade), anhydrous ethanol (Pharmco), and all other solvents (Fisher ACS Grade) were used as received. Cobalt(II) perchlorate hexahydrate, 10% palladium on activated carbon,  $\gamma$ -butyrolactone, thionyl chloride, *tert*-butyl alcohol, dibutylamine, 4-*tert*-butylpyridine, 2,2'-dipyridyl, 4,4'-diphenyl-2,2'-dipyridyl, 4,4'-di-*tert*-butyl-2,2'-dipyridyl, 4,4'-dinonyl-2,2'-dipyridyl, 4,4',4''-tri-*tert*-butyl-2,2':6',2''-terpyridine, 1,10-phenanthroline, 4,7-diphenyl-1,10-phenanthroline, silver nitrate, lithium perchlorate, lithium triflate, and nitrosonium tetrafluoroborate were purchased from Aldrich at  $\geq 97\%$  purity and used as received. 3-Methoxypropionitrile (Aldrich 98%) and 4-(3-pentyl)pyridine (TCI 95+%) were distilled under dynamic vacuum prior to use. 4,4'-Dimethyl-2,2'-dipyridyl was purchased from Reilly Industries, Indianapolis, IN. 5,5'-Dimethyl-2,2'-dipyridyl and 4,4',5,5'-tetramethyl-2,2'-dipyridyl were prepared as described previously.<sup>16</sup> All methyl-substituted bipyridines were recrystallized from ethyl acetate. 2,2'-Bipyridine-4,4'-dicarboxylic acid,<sup>17</sup> 4,4',4''-triethyl-2,2':6',2''-terpyridine,<sup>1</sup> and *cis*-di(isothiocyanato)-bis(2,2'-bipyridine-4,4'-dicarboxylic acid)ruthenium(II) (N3)<sup>18</sup> were prepared according to previously published procedures.

**Synthesis. Synthesis of 4,4'-Di-(3-pentyl)-2,2'-dipyridyl.** Freshly distilled 4-(3-pentyl)pyridine (18 mL) was refluxed with 2 g of 10% Pd on activated carbon under nitrogen for 5 days. After the mixture cooled to room temperature, the solids were filtered and rinsed with dichloromethane ( $\text{CH}_2\text{Cl}_2$ ). The solvent in the filtrate was then removed by rotary evaporation. Most of the unreacted 4-(3-pentyl)pyridine was removed by vacuum distillation. The remaining viscous oil was subjected to flash column chromatography using silica gel. The eluent was a gradient of acetone in  $\text{CH}_2\text{Cl}_2$  that was saturated with concentrated ammonium hydroxide solution. Combining and reducing the volume of the product-containing fractions resulted in 2.7 g (16% yield) of 4,4'-di-(3-pentyl)-2,2'-dipyridyl in the form of a nearly colorless viscous oil that solidified into a waxy crystalline solid on standing at room temperature.

<sup>1</sup>H NMR (300 MHz,  $\text{CDCl}_3$ )  $\delta$  ppm: 0.81 (12H, t, 4  $\times$  CH<sub>3</sub>), 1.73 (8H, m, 4  $\times$  CH<sub>2</sub>), 2.50 (2H, m, 2  $\times$  CH), 7.16 (2H, s, 2  $\times$  H5), 8.34 (2H, s, 2  $\times$  H3), 8.61 (2H, d, 2  $\times$  H6).

**Synthesis of 2,2'-Bipyridine-4,4'-dicarboxylic Acid Chloride.** Approximately 10 g of 2,2'-bipyridine-4,4'-dicarboxylic acid was placed in a 500-mL round-bottom flask fitted with a condenser. Thionyl chloride (ca. 200 mL) was added and the flask flushed with  $\text{N}_2$ . The solution was refluxed under a static  $\text{N}_2$  atmosphere with stirring for 3–4 days. The solution was allowed to cool, and the solids were allowed to settle. Approximately 50 mL of the clear yellowish solution was decanted into a clean 250-mL flask, with care taken not to transfer any of the unreacted solid. The thionyl chloride was removed by rotary evaporation, leaving a slightly yellow-green solid on the sides of the flask. This product was used immediately without characterization or further purification.

**Synthesis of 2,2'-Bipyridine-4,4'-di-*tert*-butoxyester.** From a freshly opened bottle that had previously been warmed to melt the contents, ca. 20 mL of *tert*-butyl alcohol was transferred to a clean dry Erlenmeyer flask. A piece of sodium (ca. 1 g) was washed several times with *tert*-butyl alcohol and added to the Erlenmeyer flask. The flask was warmed with stirring under  $\text{N}_2$  until the sodium had totally dissolved (ca. 1.5 h). This solution of sodium *tert*-butoxide was then added to the flask containing the 2,2'-bipyridine-4,4'-dicarboxylic acid

(12) Oskam, G.; Bergeron, B. V.; Meyer, G. J.; Searson, P. C. *J. Phys. Chem. B* **2001**, *105*, 6867.

(13) Bonhôte, P.; Grätzel, M.; Jirousek, M.; Liska, P.; Pappas, N.; Vlachopoulos, N.; Von Planta, C.; Walder, L. Presented at the 10th International Conference on Photochemical Conversion and Storage of Solar Energy (IPS-10), Interlaken, Switzerland, 1994, Abstract C2.

(14) Wen, C.; Ishikawa, K.; Kishima, M.; Yamada, K. *Sol. Energy Mater. Sol. Cells* **2000**, *61*, 339.

(15) Nusbaumer, H.; Moser, J. E.; Zakeeruddin, S. M.; Nazeeruddin, M. K.; Grätzel, M. *J. Phys. Chem. B* **2001**, *105*, 10461.

(16) Sasse, W. H. F.; Whittle, C. P. *J. Am. Chem. Soc.* **1961**, *83*, 1347.

(17) Nazeeruddin, M. K.; Kalyanasundaram, K.; Graetzel, M. *Inorg. Synth.* **1997**, *32*, 181.

(18) Nazeeruddin, M. K.; Kay, A.; Rodicio, I.; Humphry-Baker, R.; Mueller, E.; Liska, P.; Vlachopoulos, N.; Graetzel, M. *J. Am. Chem. Soc.* **1993**, *115*, 6382.

chloride. The flask immediately became hot to the touch. The resulting slurry was stirred for 30 min. and allowed to cool to room temperature. The solution was then filtered, and the solid was washed with several portions of  $\text{CH}_2\text{Cl}_2$ .

The solution fractions were combined, and the solvent was removed by rotary evaporation, leaving a yellowish solid on the sides of the flask. This solid consisted of the desired product, the monoacid-monoester bipyridine and a small amount of dicarboxylic acid bipyridine. The desired product was extracted from the solid mixture by adding several 10-mL portions of toluene to the flask and heating with swirling with a heat gun until the start of reflux. The toluene was then allowed to cool to room temperature before decanting from the solid residue. This process was repeated until the toluene no longer tested significantly positive for dissolved bipyridine (by adding several drops to a solution of  $\text{Fe}(\text{ClO}_4)_2 \cdot \text{XH}_2\text{O}$  in acetone which turns red-purple if the product is present). The toluene fractions were combined, the volume was reduced to a few milliliters, and the solution was placed in a freezer. White, waxy crystals formed and were filtered from the cold solution. The product thus obtained was pure by TLC ( $\sim 1$  g).

$^1\text{H}$  NMR (300 MHz,  $\text{CDCl}_3$ )  $\delta$  ppm: 1.65 (18H, s,  $6 \times \text{CH}_3$ ), 7.85 (2H, d,  $2 \times \text{H}_5$ ), 8.84 (2H, m,  $2 \times \text{H}_3$ ,  $2 \times \text{H}_6$ ).

**Synthesis of 2,2'-Bipyridine-4,4'-bis-(di-*n*-butylamide).** Approximately 20 mL of di-*n*-butylamine was added to a flask containing the 2,2'-bipyridine-4,4'-dicarboxylic acid chloride and the flask swirled for several minutes. After the reaction mixture cooled, approximately 100 mL of chloroform was added to the flask. This solution was extracted several times with aqueous NaOH. The organic layer was collected, dried with anhydrous sodium carbonate, and reduced to a few milliliters. The crude product was chromatographed on silica gel using a gradient of acetone in  $\text{CH}_2\text{Cl}_2$ . The product obtained by removing the chromatography solvent was a white residue that had to be scraped from the sides of the flask. Estimated yield was  $\sim 1$  g.

$^1\text{H}$  NMR (300 MHz,  $\text{CDCl}_3$ )  $\delta$  ppm: 0.81 (6H, t,  $2 \times \text{CH}_3$ ), 1.02 (6H, t,  $2 \times \text{CH}_3$ ), 1.15 (4H, two offset quintets,  $2 \times \text{CH}_2$ ), 1.43 (4H, two offset quintets,  $2 \times \text{CH}_2$ ), 1.52 (4H, quintet,  $2 \times \text{CH}_2$ ), 1.68 (4H, quintet,  $2 \times \text{CH}_2$ ), 3.20 (4H, t,  $2 \times \text{CH}_2$ ), 3.51 (4H, t,  $2 \times \text{CH}_2$ ), 7.30 (2H, m,  $2 \times \text{H}_5$ ), 8.41 (2H, s,  $2 \times \text{H}_3$ ), 8.74 (2H, m,  $2 \times \text{H}_6$ ).

**Synthesis of  $[\text{Co}^{\text{II}}(\text{L})_3]\{\text{ClO}_4\}_2$  and  $[\text{Co}^{\text{II}}(\text{L})_2]\{\text{ClO}_4\}_2$  Complexes.** All of the complexes depicted in Figure 1 were synthesized using the same procedure. Briefly, 3 equiv of a bidentate ligand or 2 equiv of a tridentate ligand was dissolved with magnetic stirring in refluxing methanol. The volume of methanol was adjusted according to the solubility of the ligand and the scale of the reaction such that all of the ligand material was dissolved. To this mixture was then added 1 equiv of cobalt(II) perchlorate hexahydrate, and the mixture was allowed to stir at reflux for 2 h. After the mixture cooled to room temperature, the total volume was reduced by ca. 80% with the use of rotary evaporation. Addition of ethyl ether caused the precipitation of the product (as a solid that varied from light brown to light yellow), which was filtered and dried under vacuum. The resulting complexes were used without any further purification.

**Dye Solutions.** Saturated solutions of N3 were prepared by adding ca. 4 mg of dye to 10 mL of dry ethanol. This mixture was sonicated for ca. 10 min and filtered to remove undissolved dye.

**Electrode Preparation.**  $\text{TiO}_2$  colloidal solutions were prepared either according to "Method A" reported by Nazeeruddin et al.<sup>18</sup> or according to the method reported by Zaban et al.<sup>19</sup> and will be referred to as the nitric acid or acetic acid preparation, respectively. Films of the colloid were coated onto  $\text{SnO}_2$ :F-coated glass electrodes (Pilkington TEC 15) using the "1 Scotch" method. Zaban et al. described this technique in detail.<sup>19</sup> After coating, the films were air-dried and then sintered in air at 450 °C for 1 h. The still hot electrodes (ca. 80 °C) were then immersed in the dye solution and allowed to sit in the dark at least

overnight. Photoanodes were kept in the dark and in the dye solution until needed. Just prior to use, they were removed from the dye solution, rinsed thoroughly with dry ethanol, and dried under a stream of nitrogen. In some cases, the photoanodes were further treated by immersion in a 0.5 M solution of 4-*tert*-butylpyridine in acetonitrile (ACN) for 10–30 min followed by rinsing in ACN just prior to use.

Platinum-on-glass electrodes, made by a sputtering process, were donated by Dr. Suzanne Ferrere at the National Renewable Energy Laboratories in Golden, Colorado. Gold-on-glass electrodes were made by thermal vapor deposition of 25 nm chromium followed by 150 nm gold on glass. Carbon-coated electrodes were made by spraying three to five coats of Aerodag G (Acheson) on  $\text{SnO}_2$ :F electrodes. The carbon coating produced in this way was very fragile, and each electrode could only be used in a cell once, as cell disassembly usually created large scratches in the carbon film.

**Mediator Preparation.** Cobalt-based mediators were created by the addition of the desired Co(II) complex at various concentrations in either methoxypropionitrile (MPN) or  $\gamma$ -butyrolactone (gBL). In all cases, the appropriate amount of nitrosonium tetrafluoroborate ( $\text{NOBF}_4$ ) was added to oxidize 10% of the added Co(II) complex. In some cases, 0.2 M 4-*tert*-butylpyridine was added to the mediator solutions. Lithium triflate or  $\text{LiClO}_4$  was also added at various concentrations to some mediator solutions. For the purposes of comparison, a standard iodide-based mediator solution was prepared that consisted of LiI and  $\text{I}_2$  (10:1) in MPN.

**Analytical Measurements.** UV–vis spectra were obtained using a HP 8452A diode array spectrophotometer. A reduced-volume, 1-cm path length, quartz cell was used for measurement of all solutions. Cyclic voltammetric data was obtained using a standard three-electrode cell with an EG&G PAR model 173 potentiostat/galvanostat controlled by a model 175 Universal Programmer. The data were recorded on a Yokogawa 3023 X-Y recorder. The reference electrode was  $\text{Ag}/\text{Ag}^+$  (0.47 V vs SHE) composed of 0.1 M silver nitrate in dimethyl sulfoxide. The auxiliary electrode was a 0.5  $\text{cm}^2$  platinum flag, and the working electrode was a glassy carbon ( $7.1 \times 10^{-2} \text{ cm}^2$ ), gold ( $7.1 \times 10^{-2} \text{ cm}^2$ ), or platinum ( $2.8 \times 10^{-2} \text{ cm}^2$ ) disk electrode (BAS). Prior to use, each working electrode was polished on a felt pad with a water slurry of 0.3  $\mu\text{m}$  alumina polishing powder, followed by rinsing and sonication in ACN. This polishing procedure was repeated before each electrochemical experiment. The supporting electrolyte was 0.1 M lithium perchlorate in ACN.

Photoaction spectra were obtained from DSSCs in a two-electrode sandwich cell arrangement. Typically, 10  $\mu\text{L}$  of electrolyte was sandwiched between a  $\text{TiO}_2$  photoanode and a counter electrode. When solutions of the different cobalt mediators (0.25 M Co(II)/0.025 M  $\text{NOBF}_4$ ) in MPN were used, the counter electrode was made of gold-sputtered on  $\text{SnO}_2$ :F-coated glass. A platinum-sputtered  $\text{SnO}_2$ :F-coated glass electrode was employed as a counter electrode when the redox mediator was 0.25 M LiI/0.025 M  $\text{I}_2$ . The cell was illuminated with a 150-W Xe lamp coupled to an Applied Photophysics high-irradiance monochromator. The irradiated area was 0.5  $\text{cm}^2$ . Light excitation was through the  $\text{SnO}_2$ :F-coated glass substrate of the photoanode. Photocurrents were measured under short circuit conditions with a Contron model DMM 4021 digital electrometer. Incident irradiance was measured with a calibrated silicon photodiode from UDT Technologies.

To test the performance of each electron-transfer mediator solution, cells were assembled by clamping together a photoanode and cathode in a specially designed cell holder having a light aperture area of 0.4  $\text{cm}^2$ . The electron-transfer mediator was introduced by the addition of a few drops of solution at the edge of the electrodes. Capillary forces were sufficient to draw the solution onto the entire electrode area. Solar illumination was simulated using the output of an Oriel 75-W xenon arc lamp which was further attenuated using neutral density filters and a 400-nm high-pass cutoff filter. The light intensity after filtering was adjusted to 100  $\text{mW cm}^{-2}$  (ca. 1 sun) at the distance of the photoanode using a Molelectron PowerMax 500A power meter. The current output

(19) Zaban, A.; Ferrere, S.; Sprague, J.; Gregg, B. A. *J. Phys. Chem. B* **1997**, *101*, 55.



**Table 1.** Spectral Properties of Representative Cobalt(II) Complexes

complex	$\lambda_{\text{max}}$ (nm)	$\epsilon_{\lambda_{\text{max}}}$ ( $\text{M}^{-1} \text{cm}^{-1}$ )	complex	$\lambda_{\text{max}}$ (nm)	$\epsilon_{\lambda_{\text{max}}}$ ( $\text{M}^{-1} \text{cm}^{-1}$ )
ttb-terpy	450	$1.4 \times 10^3$	dn-bpy	440	$1.1 \times 10^2$
dtb-bpy	440	$1.4 \times 10^2$	bdb-amd	440	$1.5 \times 10^2$
d3p-bpy	440	$1.1 \times 10^2$			

of each cell was recorded in the dark and under solar illumination while sweeping the voltage between ca. 0.8 and  $-0.2$  V using the same instrumentation as was used for cyclic voltammetry. The data thus obtained was digitized using an Acer flatbed scanner and tsEdit digitizing software on a computer running under Windows 98.

## Results and Discussion

**Ligands.** Cobalt complexes of unsubstituted and methyl-substituted bipyridine or terpyridine ligands are poor electron-transfer mediators in the type of DSSCs considered herein. In contrast, if the ligand contains a tertiary butyl substituent in the position para to each nitrogen, the resulting cobalt complex-based mediators yield cells with quite good short circuit photocurrent densities ( $J_{\text{sc}}$ ) and open circuit photovoltages ( $V_{\text{oc}}$ ). Were these substituent effects electronic in origin, then ligands substituted with methyl groups should produce similarly good mediators (*vide infra*) and they do not. Consequently, we initiated this study, assuming that the difference in mediator behavior of *tert*-butyl-substituted polypyridine ligands was related to the steric bulk of the *tert*-butyl group. Three types of polyimine ligands were examined: 2,2'-bipyridines, 1,10-phenanthrolines, and 2,2':6',2''-terpyridines. Alkyl substituents having a range of steric requirements were examined. Since the electron-donating effect of all simple alkyl substituents is essentially the same (e.g., methyl, ethyl, *tert*-butyl, etc.),<sup>20</sup> all of the complexes of a given ligand-type (i.e., bipyridine, phenanthroline, or terpyridine) were expected and found to have very similar  $E_{1/2}$  values for the relevant Co(II/III) couple. In addition, several other types of bulky substituents were examined which have significantly different electronic effects. This group included aryl substituents and strongly electron-withdrawing ester and amide groups. These latter two types of substituents make the ligands electron-deficient and produce cobalt complexes with significantly more positive  $E_{1/2}$  values; consequently, the maximum theoretically possible  $V_{\text{oc}}$  is likewise greater.<sup>11</sup>

**Spectral Properties.** All of the complexes under consideration exhibit similar UV-vis absorption spectra. Each of the Co(II) complexes has a weak absorption band centered at ca. 440–450 nm. The onset of the ligand-based  $\pi$ – $\pi^*$  transition occurs in the UV above 350–380 nm for each of the ligands. Molar extinction coefficients ( $\epsilon_{\lambda_{\text{max}}}$ ) for the band at 440–450 nm were obtained from Beer's law plots of standard solutions of each Co(II) complex. Table 1. summarizes the data for a set of representative complexes. The most intense visible absorption is for ttb-terpy<sup>2+</sup> with  $\epsilon_{450} = 1.4 \times 10^3 \text{ M}^{-1} \text{cm}^{-1}$ . The remaining complexes all exhibit  $\epsilon_{\lambda_{440-450}}$  values that are approximately an order of magnitude smaller. In all cases, the visible absorbance of the Co(III) form is almost imperceptible, and partial oxidation of solutions of any of the Co(II) complexes reduces the overall absorbance. For the sake of comparison, the  $\epsilon_{\lambda_{440-450}}$  value for  $\text{I}_3^-$  is ca.  $2 \times 10^3 \text{ M}^{-1} \text{cm}^{-1}$ ; therefore,

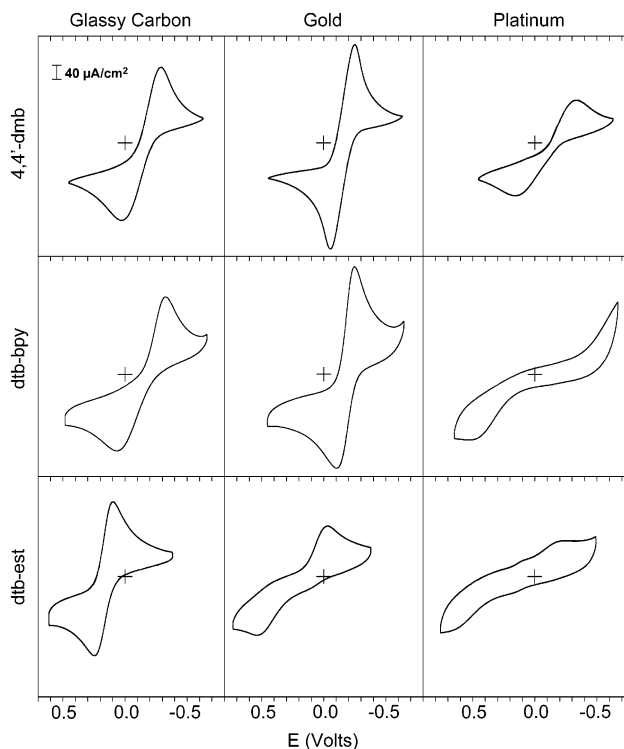


**Figure 2.** Cyclic voltammograms of three different cobalt complexes (in rows) on three different electrodes (in columns). The vertical axis is current density to compensate for modest differences in electrode areas, and the scale is indicated in the upper left-hand corner. The concentration of the complexes was  $10^{-3}$  M, and the scan rate was  $200 \text{ mV s}^{-1}$ . See the text for details.

except for ttb-terpy<sup>2+</sup> that has a comparable absorbance, considerably less visible light is absorbed by all of the remaining cobalt complexes at similar concentrations.

**Electrochemical Studies.** Electrochemical characterization of these complexes revealed a dramatic and unexpected electrode surface dependence to the electron-transfer kinetics. Each complex was examined by cyclic voltammetry on three different working electrodes: glassy carbon, gold, and platinum. Figure 2 shows nine cyclic voltammograms (CVs) representing three different complexes (rows) on the three different working electrode surfaces (columns). The vertical axis in these CVs was converted to current density to normalize for the different electrode areas. Table 2 contains the measured electrochemical parameters for the complete set of complexes.

The results found for 4,4'-dmb and dtb-bpy (Figure 2, top and middle rows, respectively) are typical of complexes with ligands containing alkyl substituents in the 4 and 4' (or equivalent) positions. Gold electrodes exhibit the most reversible and ideally shaped CVs. Glassy carbon electrodes also produce quasi-reversible voltammograms, although less reversible than gold. Quite unexpectedly, the voltammetry on platinum electrodes is quite irreversible with large anodic and cathodic peak separations ( $\Delta E_p$ ) or, in some cases, peaks that are so broad as to be indistinguishable as peaks. In contrast, the voltammetry of the dtb-est complex (Figure 1, bottom row), is most reversible on glassy carbon with  $\Delta E_p$  increasing on gold and platinum.

Complexes whose ligands are either unsubstituted or are substituted only in the 5 and 5' positions with methyl groups exhibited very different behavior (see Table 2). In general, there is a less dramatic surface dependence. Gold and platinum

(20) Wade, L. G. *Organic Chemistry*, 2nd ed.; Prentice-Hall: Englewood Cliffs, New Jersey, 1991; Chapter 17.

**Table 2.** Electrochemical Properties of Cobalt Complexes

complex	glassy carbon		gold		platinum	
	$E_{1/2}$ (mV)	$\Delta E_p$ (mV)	$E_{1/2}$ (mV)	$\Delta E_p$ (mV)	$E_{1/2}$ (mV)	$\Delta E_p$ (mV)
te-terpy	−103	200	−138	111	−140	156
ttb-terpy	−229	77	−234	75	(a)	(a)
bpy	−7	86	−10	60	−7	60
4,4′-dmb	−139	171	−149	110	−79	290
5,5′-dmb	−99	115	−103	60	−100	64
tm-dmb	−217	123	−225	57	−141	326
dtb-bpy	−139	271	−177	86	(a)	(a)
dp-bpy	−107	94	−109	69	−81	162
d3p-bpy	−58	116	−60	82	(a)	(a)
dn-bpy	−147	80	−143	76	−125	221
phen	80	198	73	87	81	153
phen-phen	−87	60	−84	75	−71	163
dtb-est	174	103	242	398	257	631
bdb-amd	217	101	222	86	291	442

<sup>a</sup> No discernible cathodic peak.

electrodes give nearly reversible voltammograms, while the CVs on glassy carbon are quasi-reversible.

In general, the shapes of the quasi-reversible waves indicate that, in cases where the heterogeneous electron transfer is slow, the transfer coefficient,  $\alpha$ , is considerably greater than 0.5.<sup>21</sup> In other words, for equivalent overpotentials the heterogeneous reduction of the Co(III) complex is considerably faster than the corresponding oxidation of the Co(II) species. While the electrode-dependent electron-transfer kinetics are not presently understood, there is a rough empirical correlation between the solution voltammetry of a complex and its performance as a redox mediator in a DSSC. The complexes that exhibit reversible or nearly reversible voltammetry on all three electrodes are generally poor mediators; that is they give very low  $J_{sc}$  values. The voltammetric results also suggest that, while platinum is the cathode of choice for the  $I^-/I_3^-$  redox mediator, it should not be the optimal choice for cobalt complex-based mediators. Likewise, while carbon is a poor cathode with the  $I^-/I_3^-$  redox mediator system, it should be acceptable for any of the cobalt systems considered here.

**Initial Screening of Mediators.** To qualitatively and quantitatively compare these cobalt complexes as mediators, DSSCs were assembled using identical photoanodes and cathodes. Due to the varying solubility of the complexes, the concentration of mediator in solution was kept low. This resulted in devices with less than optimal performance, but allowed for comparisons in cell performance as a function of mediator structure.

As with the electrochemical observations, there were distinct differences in cell performance based on the identity of the ligand substituents and in what positions they were located. Mediators based on phen, phen-phen, bpy, 5,5′-dmb, or tm-bpy yielded almost no photocurrent. Mediators composed of 4,4′-dmb and te-terpy resulted in a very modest photoeffect, but both  $V_{oc}$  and  $J_{sc}$  were very low, and further investigation with these complexes was considered unwarranted. Both dtb-est and bdb-amd gave  $V_{oc} > 0.55$  V but gave  $J_{sc}$  that were ca. <10% that of the best cobalt-based systems. The remaining complexes under consideration showed promise as potential efficient mediators, and efforts were focused on optimizing DSSCs containing the best of these.

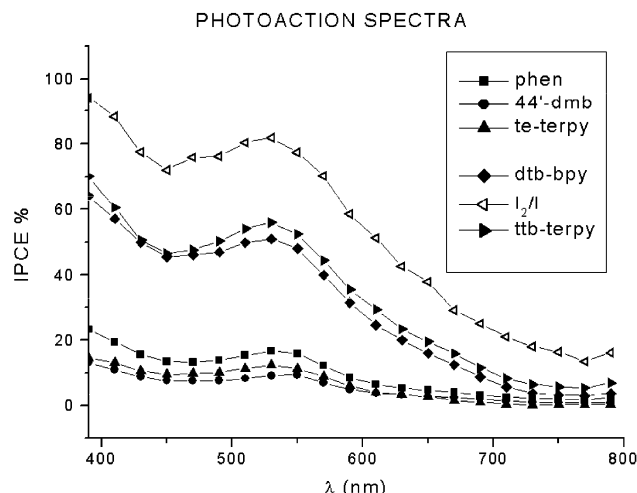


**Figure 3.** Photoaction spectra of N3 bound to nanocrystalline  $TiO_2$  films in the presence of different electron mediators in MPN solutions: 0.25 M  $LiI/25$  mM  $I_2$  (—triangle left open—), 0.25 M  $ttb\text{-}terpy^{2+}/25$  mM  $NOBF_4$  (—triangle right solid—), 0.25 M  $dtb\text{-}bpy^{2+}/25$  mM  $NOBF_4$  (—diamond—), 0.25 M  $phen^{2+}/25$  mM  $NOBF_4$  (—square—), 0.25 M  $te\text{-}terpy^{2+}/25$  mM  $NOBF_4$  (—triangle—), saturated (<0.15 M) 4,4′-dmb<sup>2+</sup>/15 mM  $NOBF_4$  (—circle—). 0.25 M  $LiClO_4$  was added to all solutions containing a cobalt mediator.

**Solvents and Cathode Materials.** In surveying a number of potential low volatility solvents, MPN and gBL were found to work well with all of the cobalt mediators. For any given concentration of mediator, gBL was generally a superior solvent, in that the fill factor (FF) was improved over the same cell made with MPN as the mediator solvent. However, in some cases the mediators were more soluble in MPN, and in those cases the higher concentration of mediator made for better cell performance.

Gold cathodes should give higher  $J_{sc}$  than platinum since, for efficient mediators, the reduction of  $Co(L)_3^{3+}$  (e.g.,  $dtb\text{-}bpy^{3+}$ , Figure 2) is much faster on gold than platinum; this was indeed found to be the case. For all the efficient cobalt complex mediators, cells assembled using gold cathodes outperformed those assembled with platinum. However, platinum gave better results than might have been anticipated from the voltammetry. In all of our studies there was no evidence that the cobalt complexes were in any way corrosive toward the gold surface. In fact, the same gold cathode was used throughout the course of these investigations, and remains unchanged.

Again, on the basis of the CV results, we anticipated that a carbon cathode should also work well in these cells. To that end we prepared cathodes consisting of  $SnO_2:F$  glass coated with a thin layer of graphite nanoparticles. These carbon-coated cathodes work well initially, even outperforming platinum, but they are not stable for extended periods because the layers of graphite particles are not held together with any binder and are readily damaged (this is especially evident when the cell is disassembled). Nevertheless, these results demonstrate the proof-of-concept that a stable carbon cathode should function well in cells based on these cobalt mediators.

**Photoaction Spectra.** Photoaction spectra—incident photon-to-current conversion efficiency (IPCE) versus wavelength—of N3 bound to nanocrystalline  $TiO_2$  films in the presence of different electron-transfer mediators in MPN solutions are shown in Figure 3. The performances of the photoelectrochemical cell are observed to be strongly dependent on the composition of the electrolyte solution. A maximum conversion efficiency of

(21) Bard, A. J.; Faulkner, L. R. *Electrochemical Methods*, 1st ed.; John Wiley & Sons: New York, 1980; Chapter 3.

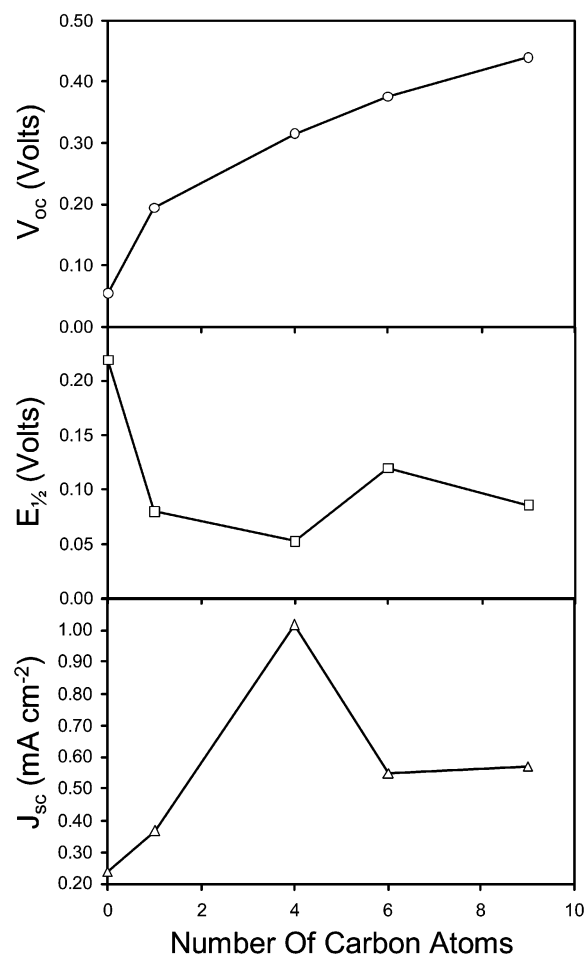


**Figure 4.** A plot of  $V_{oc}$ ,  $E_{1/2}$ , and  $J_{sc}$  as a function of the number of carbon atoms in the alkyl or aryl substituents at the 4 and 4' positions of 2,2'-bipyridine ligands.  $V_{oc}$  and  $J_{sc}$  were measured in DSSCs with a gold cathode and containing 125 mM Co(II)L<sub>3</sub> and 13 mM NOBF<sub>4</sub> in MPN.

ca. 80%, in correspondence to the metal-to-ligand charge-transfer absorption maximum of N3 was obtained in the presence of 0.25 M LiI/0.025 M I<sub>2</sub>. With the cobalt complex mediators, the best performances were observed when solutions of ttb-terpy<sup>2+</sup>/ttb-terpy<sup>3+</sup> (ca. 55% IPCE) and dtb-bpy<sup>2+</sup>/dtb-bpy<sup>3+</sup> (ca. 50% IPCE) were used. In the other investigated cases, the phen, te-terpy, and 44'-dmb complex-based mediators exhibited maximum IPCE values in the range of 10–20%.

**Open-Circuit Voltage.** Figure 4 shows  $V_{oc}$ ,  $E_{1/2}$ , and  $J_{sc}$  data for five different cobalt bipyridine mediators plotted against the number of carbons in the substituents. In each case, the substituent is either an aryl or alkyl group that is appended at the 4 and 4' positions. These measurements were all made using MPN as the solvent. The mediators were all 125 mM in Co(II)L<sub>3</sub> and 13 mM in Co(III)L<sub>3</sub>, and nothing else was added to the solution (i.e., no other cations were present, and the solution contained no pyridine-type bases). It is interesting that, within this limited set of complexes at least, there is no obvious correlation between  $V_{oc}$  and  $E_{1/2}$ . On the other hand, there is a steady increase in the value of  $V_{oc}$  with the number of carbons in the ligand's substituents, which appears to be asymptotically approaching a limiting value. In the most generally accepted description,<sup>11,22,23</sup>  $V_{oc}$  is the difference of the quasi-Fermi level

of electrons at the negative electrode and the “holes” at the positive electrode. This latter term is essentially the Nernstian potential of the cobalt couple at the cathode. All of the 4,4'-alkyl- and 4,4'-aryl-substituted bipyridine complexes herein have similar  $E_{1/2}$  (within ca. 60 mV), so that they should all yield the same  $V_{oc}$ , all else being equal. The fact that  $V_{oc}$  varies by ca. 400 mV over this collection of mediators indicates that something must shift the Fermi energy of the electrons in the TiO<sub>2</sub>. The two most obvious candidates are shifts in the conduction band edge of the TiO<sub>2</sub> or differences in the rates of electron/Co(III)L<sub>3</sub> recombination. With I<sup>−</sup>/I<sub>3</sub><sup>−</sup>, numerous studies have demonstrated that  $V_{oc}$  depends on the size of the counter-cation of iodide.<sup>24–26</sup> This effect is ascribed to a shift in the conduction band edge energy of TiO<sub>2</sub> upon adsorption, or intercalation of cations, and the magnitude of this shift is related to the charge-to-radius ratio of the cation. The complexes considered in Figure 4 are of different sizes, and the trend in  $V_{oc}$  is in the correct direction to be consistent with this model (i.e.,  $V_{oc}$  increases with larger radius). Furthermore, Nusbaumer et al. have shown that a related cobalt complex-based mediator does adsorb on the TiO<sub>2</sub> surface.<sup>15</sup> While this picture is in qualitative agreement with the model, it does not stand up to a more quantitative analysis. With I<sup>−</sup>/I<sub>3</sub><sup>−</sup>, the typical shift in  $V_{oc}$  upon changing between Li<sup>+</sup> and Cs<sup>+</sup> is less than 200 mV (at comparable concentrations), while their ionic radii differ by almost a factor of  $\times 3$ .<sup>25</sup> The difference in  $V_{oc}$  between bpy- and dn-bpy-mediated cells is ca. 400 mV, but their radii differ by, at most, a factor  $\times 2$ . More likely the variations in  $V_{oc}$  arise from differences in the recombination rate between Co(III)L<sub>3</sub> and photoinjected electrons, which should decrease as the bulk of the substituents increases (vide infra).

**Lithium Ion Effect.** As considered above, the presence of small counter-cations (most notably Li<sup>+</sup>) in mediator solutions of I<sup>−</sup>/I<sub>3</sub><sup>−</sup> lowers  $V_{oc}$ . Concomitantly,  $J_{sc}$  increases, and the net result is an overall improvement in cell efficiency ( $\eta$ ).<sup>24</sup> There is ample experimental verification that adsorbed Li<sup>+</sup> lowers the energy of acceptor states in the TiO<sub>2</sub>, and this fact is the most commonly invoked explanation for the cation-induced decrease in  $V_{oc}$ .<sup>24</sup> The origin of the increased  $J_{sc}$  upon addition of Li<sup>+</sup> to the I<sup>−</sup>/I<sub>3</sub><sup>−</sup> is less clear. Photoinjection of electrons from the excited dye occurs with near unity quantum efficiency irrespective of the cation. Since the photocurrent is determined by the difference between the photoinjection rate and the overall recombination rate, any increase in  $J_{sc}$  must lie in cation-induced changes in recombination rates (irrespective of the type of mediator system).

In principle, Li<sup>+</sup> could decrease recombination in at least three ways: (1) by accelerating the rate of oxidized dye reduction by I<sup>−</sup>, (2) by slowing the rate of direct combination of electrons with the dye, or (3) by slowing the rate of recombination of electrons with I<sub>3</sub><sup>−</sup>. Grätzel et al. showed that Li<sup>+</sup> (and other cations with high charge-to-radius ratios) greatly accelerates the rate of reaction between I<sup>−</sup> and adsorbed photooxidized N3.<sup>27</sup> In practice, for the I<sup>−</sup>/I<sub>3</sub><sup>−</sup> system this is largely irrelevant to  $J_{sc}$

(22) Cahen, D.; Hodes, G.; Graetzel, M.; Guillemoles, J. F.; Riess, I. *J. Phys. Chem. B* **2000**, *104*, 2053.

(23) Huang, S. Y.; Schlichthorl, G.; Nozik, A. J.; Gratzel, M.; Frank, A. J. *J. Phys. Chem. B* **1997**, *101*, 2576.

(24) Kelly, C. A.; Farzad, F.; Thompson, D. W.; Stipkala, J. M.; Meyer, G. J. *Langmuir* **1999**, *15*, 7047.

(25) Liu, Y.; Hagfeldt, A.; Xiao, X. R.; Lindquist, S. E. *Sol. Energy Mater. Sol. Cells* **1998**, *55*, 267.

(26) Enright, B.; Redmond, G.; Fitzmaurice, D. J. *Phys. Chem.* **1994**, *98*, 6195.

(27) Pelet, S.; Moser, J.-E.; Graetzel, M. *J. Phys. Chem. B* **2000**, *104*, 1791.



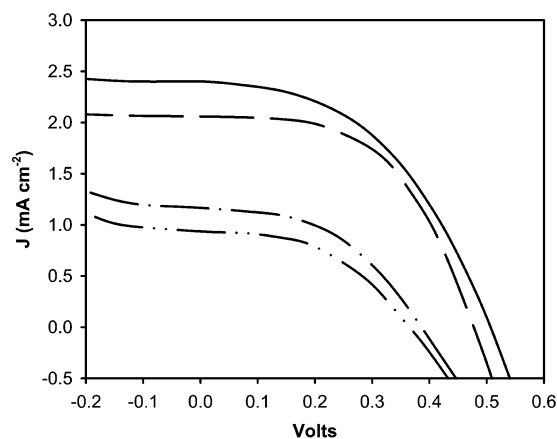


**Figure 5.** Current–voltage response of DSSCs with a gold cathode and containing: 0.25 M dtb-bpy and 25 mM NOBF<sub>4</sub> in gBL (···), with added 0.2 M 4-*tert*-butylpyridine (– · –), with added 0.2 M 4-*tert*-butylpyridine and 0.2 M lithium triflate (—), and with added 0.2 M 4-*tert*-butylpyridine and 0.5 M lithium triflate (—).

because, at usual I<sup>−</sup> concentrations, the rate of reaction between oxidized N3 and I<sup>−</sup> is fast even in the absence of Li<sup>+</sup>.<sup>27</sup> Consequently, neither process (1) nor (2) above should be a significant factor in determining  $J_{sc}$ , which leaves the recombination reaction of electrons with I<sub>3</sub><sup>−</sup> as the dominant factor. The Li<sup>+</sup>-induced lowering of the acceptor-state energies in the TiO<sub>2</sub> could result in a driving-force-based decrease in the rate of I<sub>3</sub><sup>−</sup> reduction at the photoanode. Alternately, and most probably, adsorbed cations affect the rate or mechanism or both of the heterogeneous electron transfer in some undetermined way.

The addition of Li<sup>+</sup> to solutions of the cobalt-based mediators also increases  $J_{sc}$  significantly, and Figure 5 shows the current–voltage response of cells demonstrating this effect. The analogous three processes considered above remain relevant. In the discussion of  $V_{oc}$  below, data is presented that strongly indicate that Li<sup>+</sup> has a marked effect on the recombination rate with Co(III)L<sub>3</sub>. Quite possibly this is the dominant process which determines both  $J_{sc}$  and  $V_{oc}$ . However, there are presently insufficient data to totally eliminate the other two processes from consideration.

In clear contrast to I<sup>−</sup>/I<sub>3</sub><sup>−</sup>, Li<sup>+</sup> increases  $V_{oc}$  with all of the efficient cobalt mediators. It seems highly unlikely that the presence of the cobalt complex in solution would alter the effect of Li<sup>+</sup> in lowering the energy of the TiO<sub>2</sub> acceptor states (conduction band or surface states). Consequently, the Li<sup>+</sup>-induced increase in  $V_{oc}$  must come from some other source. Moreover, the effect must be large enough to offset the band shift to lower energy. First, Li<sup>+</sup> has a negligible effect on the  $E_{1/2}$  of the Co(II/III)L<sub>3</sub> couple at the cathode so that cannot be the origin of the increase in  $V_{oc}$ . As with the increase in  $J_{sc}$ , the remaining obvious possibilities are directly tied to the recombination processes discussed at the beginning of this section.

Even though the rate of oxidized N3 regeneration by I<sup>−</sup> appears to not play a significant role in recombination,<sup>27</sup> the rate of regeneration is greatly increased by the presence of Li<sup>+</sup> (vide supra). At present for our cobalt complex mediators, there are no data on how Li<sup>+</sup> affects the relative rates of reaction between the oxidized N3 dye and either the photoinjected electron or Co(II)L<sub>3</sub>. Therefore, just as in the consideration of  $J_{sc}$ , these processes cannot be discounted in terms of their

potential effect on  $V_{oc}$ . Given that caveat, there is evidence that the recombination reaction at the SnO<sub>2</sub>:F contact is affected by Li<sup>+</sup>. On a bare SnO<sub>2</sub>:F electrode of the same type used as the TiO<sub>2</sub> current collector, the overpotential for dtb-bpy<sup>3+</sup> reduction is several hundred millivolts more negative in the presence of 0.25 M Li<sup>+</sup> and 0.10 M tetrabutylammonium ion (TBA<sup>+</sup>) than in 0.10 M TBA<sup>+</sup> alone. It is also reasonable that the rate of the analogous reaction on TiO<sub>2</sub> might respond to Li<sup>+</sup> likewise, given the approximate similarity of their surfaces. Simple double-layer theory arguments predict that the specifically adsorbed cations should reduce the rate of heterogeneous reduction of a cationic mediator. Furthermore, while not conclusive, considerations of the dark current of a cell having dtb-bpy as the mediator supports this argument. For example, the dark current for the reduction of dtb-bpy<sup>3+</sup> is approximately the same magnitude at the  $V_{oc}$  with Li<sup>+</sup> present as it is at the lower  $V_{oc}$  in the absence of Li<sup>+</sup>. Put another way, the effective overpotential for this reduction in the dark increases by an amount roughly equal to the shift in  $V_{oc}$  upon addition of Li<sup>+</sup> to solution.

In a sense, the response to Li<sup>+</sup> of DSSCs with these cobalt mediators is more intuitive than with I<sup>−</sup>/I<sub>3</sub><sup>−</sup>. Decreasing the recombination rate by any mechanism should increase both  $V_{oc}$  and  $J_{sc}$ . Consequently, if  $J_{sc}$  increases, so should  $V_{oc}$ , all else being equal. The apparent conundrum is with the I<sup>−</sup>/I<sub>3</sub><sup>−</sup> system. There, the effect of the decrease in the recombination rate is insufficient to offset the shift in the conduction band, which on the surface gives rise to the intuitive contradiction.

**Pyridine Effect.** The effect on  $V_{oc}$  of adding 4-*tert*-butylpyridine to a cobalt mediator solution parallels the behavior with the I<sup>−</sup>/I<sub>3</sub><sup>−</sup> mediator system—a modest improvement results. As is evident from Figure 5, there is also a small increase in  $J_{sc}$  that is not typical of the I<sup>−</sup>/I<sub>3</sub><sup>−</sup> mediator system.<sup>23</sup> When both 4-*tert*-butylpyridine and Li<sup>+</sup> are present in solution, the increase in  $V_{oc}$  is significantly greater than for either alone (see Figure 5). The effect of added 4-*tert*-butylpyridine on the energy of the conduction band and any other acceptor states in the TiO<sub>2</sub> is anticipated to be the same as with I<sup>−</sup>/I<sub>3</sub><sup>−</sup>. Additionally, the same effect was observed whether the 4-*tert*-butylpyridine was added directly to the mediator solution or whether the photoanode was pretreated by soaking in a solution of it.

**Optimized Mediators.** To fabricate DSSCs with more optimal performance—that is, higher  $\eta$  and FF—the composition and concentration of the more promising mediators were surveyed. For dtb-bpy, d3p-bpy, and dp-bpy we found that optimal mediators were formed from saturated solutions of the corresponding Co(II) complexes and 0.5 M lithium triflate. The solubility limit in gBL is less than 0.5 M for dtb-bpy and less than 0.3 M for d3p-bpy and dp-bpy in MPN. The oxidized forms of these complexes are considerably less soluble than the corresponding Co(II) complexes under these conditions, and oxidation of 10% of the saturated solutions led to precipitation of an unknown but minimal amount of the Co(III) complex.

The dn-bpy- and ttb-terpy-based mediators show optimal performance at less than saturated concentrations. That is to say, above ca. 0.3 M, addition of more mediator actually lowers the  $\eta$  of a cell, but it is likely that there is a different explanation in each case. For dn-bpy, addition of the complex causes a dramatic increase in the viscosity of the mediator solution, much more so than for any of the other mediators under study. The



**Table 3.** Photoelectrochemical Properties of DSSCs Containing Optimized Cobalt Complex-Based Mediators

mediator <sup>a</sup>	solvent	$V_{oc}$ (volts)	$J_{sc}$ (mA cm <sup>-2</sup> )	FF (%)	$\eta^b$ (%)	$\eta_{rel}^c$ (%)
0.25 M dn-bpy, 0.25 M LiTriflate	gBL	0.43	0.89	59	0.22	31
0.25 M dp-bpy, 0.2 M LiClO <sub>4</sub>	MPN	0.40	0.97	49	0.19	27
0.25 M ttb-terpy, 0.5 M LiTriflate	MPN	0.40	1.71	48	0.32	45
0.2 M d3p-bpy, 0.2 M LiClO <sub>4</sub>	MPN	0.47	1.47	59	0.41	58
0.25 M dtb-bpy, 0.5 M LiTriflate	gBL	0.51	2.40	47	0.57	80
0.25 M LiI, 0.03 M I <sub>2</sub>	MPN	0.60	2.03	58	0.71	—
satd. dtb-bpy, 0.5 M LiTriflate <sup>d</sup>	gBL	0.44	4.82	62	1.30	82
0.5 M LiI, 0.05 M I <sub>2</sub> <sup>d</sup>	MPN	0.57	5.32	52	1.58	—

<sup>a</sup> The concentrations of complex given are for the total cobalt; each solution is 9:1 Co(II):Co(III). A gold cathode was used for all cells containing cobalt complex mediators; a platinum cathode was used in I<sup>-</sup>/I<sub>3</sub><sup>-</sup> mediated cells. These mediator solutions also contained 0.2 M 4-*tert*-butylpyridine (see “d” below for exceptions). <sup>b</sup> All efficiency measurements were carried out under 100 mW cm<sup>-2</sup> (~1 sun) illumination. <sup>c</sup> This is the efficiency relative to a comparable I<sup>-</sup>/I<sub>3</sub><sup>-</sup> mediated cell. <sup>d</sup> The photoanodes in these cells were constructed with acetic acid-prepared TiO<sub>2</sub> and, after dyeing, were soaked in 0.2 M 4-*tert*-butylpyridine in ACN just prior to use.

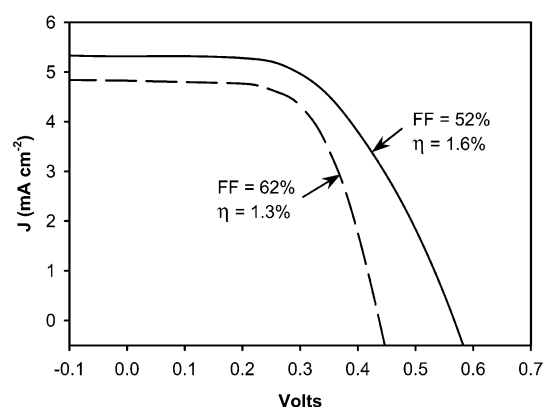


**Figure 6.** Current–voltage response of DSSCs assembled from N3-dyed photoanodes of acetic acid prepared TiO<sub>2</sub>. These photoanodes were treated with a solution 0.5 M 4-*tert*-butylpyridine in ACN just prior to use. The solid line represents a mediator of 0.5 M LiI and 50 mM I<sub>2</sub> in MPN using a platinum cathode. The dashed line represents a mediator of saturated (<0.5 M) dtb-bpy, 50 mM NOBF<sub>4</sub>, and 0.5 M lithium triflate in gBL using a gold cathode.

self-exchange rates of cobalt complexes of this type are known to be slow;<sup>28,29</sup> thus, it is safe to assume that the process of mediation is diffusion-controlled. Under high-viscosity conditions, this diffusional transport of mediator between dye-sites and the cathode is hindered and thus could become the limiting factor in determining  $J_{sc}$ . This is consistent with the behavior observed, that is, as the concentration of dn-bpy is increased,  $J_{sc}$  first increases, then decreases. For cells containing a ttb-terpy-based mediator, similar behavior is observed; however, we believe the peaking of  $J_{sc}$  values is due to the high  $\epsilon_{\lambda_{max}}$  observed for this complex—and since viscosity is not significantly different even at high concentrations of mediator. Above ca. 0.3 M, the benefit of having additional mediator is outweighed by the reduction in the amount of light reaching

the entire thickness of the photoanode; the ttb-terpy mediator simply begins to out-compete the dye for light.

Table 3 lists the data obtained for DSSCs fabricated using “optimized” cobalt mediators and comparable I<sup>-</sup>/I<sub>3</sub><sup>-</sup> mediators. All the cobalt complex-mediated cells suffer from a  $V_{oc}$  that is 100–200 mV less than that with the comparable I<sup>-</sup>/I<sub>3</sub><sup>-</sup> mediated cells. Nonetheless, the performance of these cells is still quite good, and the  $\eta$  relative to that for a comparable I<sup>-</sup>/I<sub>3</sub><sup>-</sup> mediated cell ( $\eta_{rel}$ ) is greater than 50% for d3p-bpy- and dtb-bpy-mediated cells. Cells containing the dtb-bpy-based mediators have exhibited the best performance to date, and Figure 6 shows the current–voltage response of such a cell, which exhibits a FF of 62% and  $\eta_{rel}$  of 82%.

## Conclusions

The results that we have obtained to date indicate that cobalt complexes of relatively simple and commercially available alkyl-substituted polypyridines are promising electron-transfer mediators for use in DSSCs. Cyclic voltammetric studies have shown a dramatic surface dependence of the electron-transfer kinetics, which empirical evidence suggests is a necessary attribute for an efficient mediator. The electrochemical results also led to the discovery that gold and carbon outperform platinum as cathode materials in these cells. Furthermore, these mediators show no tendency to be corrosive, enabling the use of metallized SnO<sub>2</sub>:F electrodes required in large-area DSSCs.<sup>10</sup>

Photoelectrochemical measurements of cobalt complex-mediated cells revealed that addition of lithium salts dramatically improves their performance. We have concluded that the Li<sup>+</sup> effect observed with these mediators—in contrast to I<sup>-</sup>/I<sub>3</sub><sup>-</sup> mediated cells where  $V_{oc}$  decreases instead of increasing—is due primarily to a reduction in the recombination rate between Co(III)L<sub>3</sub> and the electrons in TiO<sub>2</sub>, the SnO<sub>2</sub>:F collector, or both. Several of the complexes studied were found to be efficient mediators with dtb-bpy being the best among these. This is a particularly significant discovery because the best performing of these complexes can be made in one step from commercially available reagents without the need for further purification.

Besides being nonvolatile, noncorrosive, and lightly colored, there is an inherent advantage with cobalt complex mediators that the I<sup>-</sup>/I<sub>3</sub><sup>-</sup> mediator lacks; they can be easily modified. This research represents our first efforts to understand this new class of electron-transfer mediator. As we continue to modify, study, and improve these cobalt complex mediators, the realization of truly inexpensive, stable, and efficient DSSCs grows nearer.

**Acknowledgment.** Financial support for this research was provided by (C.M.E.) the U.S. Department of Energy, Office of Science (DE-FG03-97ER14808), and the National Science Foundation (CHE-0139637 and CHE-9714081) and by (C.A.B.) the Ferrara Research Association (F/BGI/BGI/11/01) and the Consortium Spinner (574/01). We gratefully acknowledge Drs. Suzanne Ferrere and Brian Gregg for their valuable discussions, donation of materials, and guidance in fabricating and characterizing DSSCs.

JA027355Y

(28) Szalda, D. J.; Creutz, C.; Mahajan, D.; Sutin, N. *J. Phys. Chem.* **1983**, *22*, 2372.

(29) Newton, M. D. *J. Phys. Chem.* **1991**, *95*, 30.